Colloids and Surfaces B: Biointerfaces 103 (2013) 136–142

Contents lists available at SciVerse ScienceDirect

Colloids and Surfaces B: Biointerfaces

journal homepage: www.elsevier.com/locate/colsurfb

Evaluation of antibacterial effects of carbon nanomaterials against copper-resistant *Ralstonia solanacearum*

Xiuping Wang, Xueqin Liu, Heyou Han*

State Key Laboratory of Agricultural Microbiology, College of Science, Huazhong Agricultural University, Wuhan, 430070, PR China

ARTICLE INFO

Article history:
Received 6 March 2012
Received in revised form
28 September 2012
Accepted 28 September 2012
Available online 23 October 2012

Keywords:
Carbon nanomaterials
Ralstonia solanacearum
Antibacterial activity and mechanism
Membrane disruption

ABSTRACT

In this paper, we investigated the antibacterial activity and the action mode of carbon nanomaterials (CNMs) against the copper-resistant plant pathogenic bacterium *Ralstonia solanacearum* (*R. solanacearum*). Single-walled carbon nanotubes (SWCNTs) dispersion was found to show the strongest antibacterial activity, sequentially followed by graphene oxide (GO), multi-walled carbon nanotubes (MWCNTs), reduced graphene oxide (rGO) and fullerene (C_{60}). Our investigation of the antibacterial mechanism of SWCNTs and GO indicated that the damage to the cell membrane leads to the release of cytoplasm materials from the bacterium, which is the causative factor for the inactivation of *R. solanacearum* bacterial cells. The superior antibacterial effect, and the novel antibacterial mode of SWCNTs and GO suggest that those carbon nanomaterials may have important applications in the control of plant bacterial diseases.

1. Introduction

Bacterial wilt caused by *Ralstonia solanacearum* (*R. solanacearum*) affects a large number of important crops during the growing season and throughout the postharvest storage [1]. Currently, the measures in plant protection against the bacterium are mainly based on copper derivatives, antibiotics and quaternary ammonium compounds [2]. However, with the use of these chemicals, most bacterial pathogens have developed numerous defense mechanisms against antimicrobial agents and built up resistance to commercial pesticides [3]. Especially, in recent years, the copper-resistant and streptomycin-resistant strains of the phytopathogens are widespread [4]. On the other hand, environmental pollution caused by these bactericides raised much public concern and relatively complex processing also limited the values of these compounds in crop protection [5]. Current integrated management strategies include the use of resistant cultivars, pathogen-free transplants and crop rotation with non-host cover crops [6], yet little effort has been made to control *R. solanacearum* by means of cultural management [7]. In view of the limitations of current control measures, the severe impact of bacterial wilt on important economic crops and the increase of microorganisms resistant to current pesticides, it is essential and urgent to develop an alternative agent to control the disease effectively.

In recent years, several studies have been conducted on the application of carbon nanomaterials (CNMs), especially on their antibacterial properties [8]. Two previous studies have reported that single-walled carbon nanotubes (SWCNTs) and multi-walled carbon nanotubes (MWCNTs) present a noticeable antimicrobial activity to both gram-positive bacteria and gram-negative bacteria [9,10]. GO and reduced graphene oxide (rGO) nanosheets could effectively inhibit the growth of *Escherichia coli* (*E. coli*) bacterium while showing minimal cytotoxicity to A549 cells [11]. Additionally, CNMs have been studied as possible candidates for biomedical applications, mainly because of the chemical inertness and natural presence of this element in human body [12]. For instance, SWCNTs and GO also show promise in the application of wound healing to prevent infection, allow oxygen to the wound site and stimulate the nervous and tissue growth [13]. Moreover, preferentially attacking pathogenic bacteria without adverse effects on their host is difficult. Our previous studies demonstrated the positive effects of MWCNTs and GO on germination and growth of wheat plants, and another report confirmed that CNTs can enhance the growth of tomato plants [14,15]. Furthermore, CNMs have not been shown to cause bacterial resistance and exhibit multi-point antibacterial mechanisms by rupturing bacterial wall, generating oxidative stress and inhibiting the cell growth. SWCNTs puncture bacterial cells and damage the cell membrane [16], while C_{60} exerts oxidative stress to inactivate cells [17]. Thus, CNMs possess a variety of desirable antibacterial properties, including (i) having a broad spectrum of antibacterial activity in the prevention/treatment of an infection; (ii) being nontoxic to many hosts; and (iii) being unsusceptible to the development of microbial resistance. These observations

* Corresponding author. Tel.: +86 27 87288246; fax: +86 27 87288246.
E-mail address: hyhan@mail.hzau.edu.cn (H. Han).

0927-7765/$ – see front matter.
http://dx.doi.org/10.1016/j.colsurfb.2012.09.044

highlight the importance of investigating the antibacterial properties of CNMs against plant pathogenic bacteria. However, to the best of our knowledge, few studies have documented the antimicrobial activity and mechanism of CNMs against plant pathogenic bacteria in plant protection.

In this study, we used *R. solanacearum* with copper resistance as a representative pathogenic bacterium to investigate the antibacterial properties of CNMs in three steps: first, the antibacterial activity of CNMs against *R. solanacearum* was explored by examining the OD growth curves; next, the activities of cells treated with CNMs were examined by quantifying the reduction in viable cell count and live/dead viability assay and finally, the mechanism of antibacterial activity of CNMs was investigated by SEM and TEM. Our results show that CNMs possess antibacterial activity against *R. solanacearum* and can be used as a new type of antibacterial agent to control plant bacterial diseases.

2. Materials and methods

2.1. Chemicals and bacteria

C_{60} (purity: >99.9%) products were purchased from Sigma–Aldrich. The SWCNTs and MWCNTs were purchased from Shenzhen Nanotech Port Co., Ltd. (China). SWCNTs (purity: >99%, OD × length 1–2 nm × 30 μm, —COOH content: 2.83 wt%), MWCNTs (purity: >99%, OD × length <8 nm × 30 μm, —COOH content: 3.86 wt%). All the CNMs were dispersed in water at a concentration of 1 mg/mL, and diluted in water to a desired concentration when needed. All experiments were carried out at room temperature; all solutions were prepared using de-ionized (DI) water. *R. solanacearum* was purchased from the State Key Laboratory of Agricultural Microbiology of Huazhong Agricultural University.

2.2. Preparation and characterization of GO and rGO

GO was synthesized from graphite power according to a modified Hummers method [18]. The obtained GO was reduced to rGO by using hydrazine hydrate [19]. UV–vis spectra of GO and rGO were acquired on the Nicolet Evolution 300 UV–vis spectrometer coupled with a 1.00 cm quartz cell. The thermogravimetric analysis (TGA) curves of GO and rGO were tested using a NETZSH TG209C thermobalance from room temperature to 700 °C at a heating rate of 20 K/min under N_2. TEM was carried out on Tecnai G20 microscopy (FEI, Czech) with an accelerating voltage of 200 kV.

2.3. Antimicrobial test

The antimicrobial activity of the CNMs was evaluated by examining the OD growth curves as follows. *R. solanacearum* cells were grown in Luria–Bertani (LB) broth at 30 °C and were harvested at the log phase of the growth curve. The cells were collected by centrifugation at 6000 rpm for 2 min and washed twice with sterile distilled water. Then the cells were resuspended in water, 0.9% NaCl and 0.1 M PBS (pH 7.0), respectively. Cell suspensions were adjusted to a concentration of 10^7–10^8 cfu/mL. After that, 200 μL cell suspension and 20 μL CNMs suspension were mixed and incubated at a 20 rpm shaking speed for 2 h at room temperature. Control samples contained 200 μL of the cell suspensions mixed with 20 μL of DI water. After 2 h treatment, the mixtures in the tubes were transferred into 2 mL of LB broth. The *R. solanacearum* samples were then incubated at 30 °C in an incubator with constant agitation at 120 rpm. Growth rates and bacterial concentrations were determined by measuring the optical density (OD) at 600 nm every 30 min [16].

2.4. Measurements of bacterial activity

After the *R. solanacearum* cells were treated with CNMs, the reduction in viable cell number was determined by a colony-forming units (CFU) method. The *R. solanacearum* cells were incubated in corresponding solutions containing different concentrations of CNMs, with a final cell concentration of 10^8 cfu/mL. The mixture was incubated with gentle shaking for 2 h at 30 °C. Twenty microlitres of serial 10^6-fold dilutions with corresponding buffer solutions was spread onto LB plates and left to grow for 48 h at 30 °C. Colonies were counted and compared with control plates to calculate the survival rate. Each treatment was prepared in triplicate and the mean values were compared. Survival rate% = counts of samples incubated with CNMs/counts of control [20].

2.5. Fluorescence imaging

The survival rates obtained in the CFU method were further verified by the live/dead viability after incubation with CNMs dispersions. Propidium iodide (PI, Sigma–Aldrich) and 4′-6-diamidino-2-phenylindole (DAPI, Sigma-Aldrich) were used to assess the cytotoxity of CNMs. The dye was used according to the protocol of a previous report [16]. Briefly, exponentially growing cells were diluted to an OD600 of 0.2 in water, and then 1 mL cells were treated with 100 mL different concentrations of SWCNTs and GO and incubated at 30 °C for 2 h. Then the cells were harvested by centrifugation in a microcentrifuge at 6000 rpm and resuspended in 1 mL of water before they were stained with PI (50 μg/mL) and DAPI (3 μg/mL) for 15 minutes and 5 minutes in the dark, respectively. Fluorescence images were taken on an Olympus BX40 fluorescence microscope during a single batch experiment at 400x magnification.

2.6. Integrity of cell membranes and observation of cell morphology

R. solanacearum cells were treated with 250 μg/mL of SWCNTs and GO, respectively. Then, the mixed suspensions were immediately filtered with 0.22 μm syringe filters to remove the CNMs and bacteria. The efflux of cytoplasmic materials of the cells were measured with UV–vis absorption spectroscopy at 260 nm. The morphological changes of *R. solanacearum* cells were further investigated by SEM (JEOL JSM-6700F) and TEM examination after being treated by SWCNTs and GO. Bacterial suspensions were condensed by centrifugation at 6000 rpm, and were fixed with 2.5% glutaraldehyde, before being washed with 0.1 mol/L, pH 7.0 phosphate buffers and postfixed in 1.0% osmium tetroxide. After fixation, tissues were dehydrated in an ascending ethanol series, and embedded in Spurr's resin. Finally, the thin sections containing the cells were mounted on copper grids for SEM and TEM examination [9,21].

3. Results and discussion

3.1. Characterization of GO and rGO

To investigate the effect of the reduction process of the GO, the UV-vis absorption spectroscopy was used to perform a general characterization of the graphene-based materials. The UV–vis absorption spectra showed that the absorption peak (228 nm) of GO is attributed to $\pi \rightarrow \pi^*$ transitions of aromatic C=C bonds, and gradually red-shifts to 267 nm after being reduced by hydrazine hydrate (Fig. S1A). An increase in the absorption in the whole spectral region (>248 nm) indicated that electronic conjugation has been restored within the graphene nanosheets [22].

Shown in Fig. S1B are the thermogravimetric analysis (TGA) curves of GO and rGO. For the thermal decomposition of GO, the

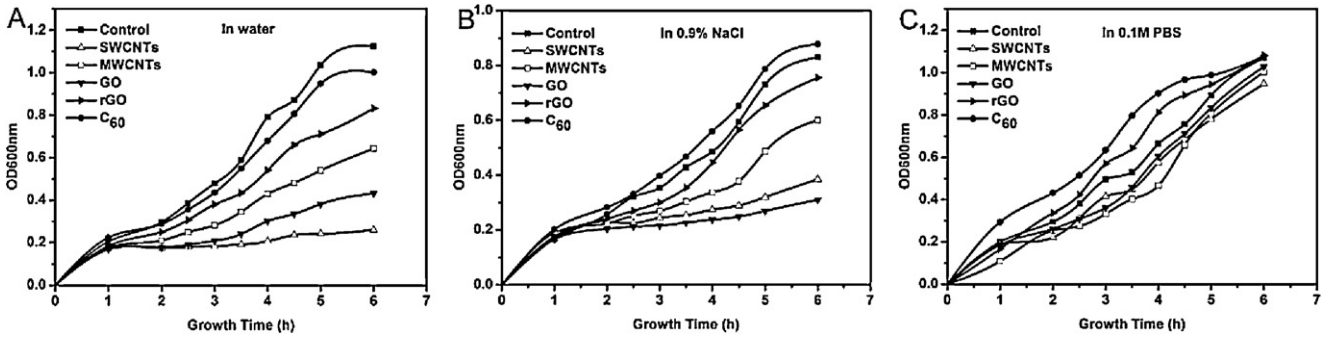

Fig. 1. OD growth curves of *R. solanacearum* in LB broth at 30 °C after the cells (200 μL, 1.2×10^7 cfu/mL) were treated with 250 μg/mL of SWCNTs, MWCNTs, GO, rGO and C_{60}, respectively, in different buffers for 2 h: (A) in water, (B) in 0.9% NaCl, and (C) in pH 7.0, 0.1 M PBS. All treatments with CNMs were performed at room temperature. All concentrations of CNMs referred to the final concentration in the treatment solutions. Controls were cells untreated with CNMs.

mass loss (10%) at the temperature range below 100 °C can be attributed to the removal of adsorbed water, whereas the steep loss (50%), which occurs around 200 °C, can be assigned to the decomposition of labile oxygen functional groups. On the other hand, a gradual mass loss (19%) over the whole temperature range from 100 °C to 700 °C after reduction indicates that the oxygen functional groups of rGO are largely removed by chemical reaction, thus showing much increased thermal stability [23].

To further characterize the exact structures of GO and rGO in the dispersions, we conducted TEM analysis (Figs. S1C and S1D). As shown in Fig. S1C, a lot of transparent and well-dispersed plates of GO can be seen to be situated on the top of the grid. The dispersion of rGO is different from that of GO (Fig. S1D), because the oxygen functional groups were reduced by hydrazine hydrate and the rGO sheets became hydrophobic, enabling us to observe the stacked and aggregated rGO layers [19].

3.2. Antibacterial activity of CNMs against R. solanacearum cells

To determine whether CNMs could be employed to inhibit the growth of or kill plant pathogenic bacteria like bacterial wilt of *R. solanacearum*, we first investigated the antimicrobial activity of CNMs (SWCNTs, MWCNTs, GO, rGO and C_{60}) against *R. solanacearum* in different buffers by examining their OD growth curves after treating the cells with the CNMs.

Shown in Fig. 1A–C are the OD growth curves of *R. solanacearum* incubated with aqueous dispersions of CNMs in water, 0.9% NaCl, and 0.1 M PBS, respectively. From Fig. 2A, a growth delay in 6 h could be observed in the *R. solanacearum* cells treated with 250 μg/mL of MWCNTs and rGO. The OD growth curves of *R. solanacearum* cells treated with 250 μg/mL of C_{60} are similar to those of the control, which suggested that C_{60} possesses no antibacterial activity against *R. solanacearum*. However, the bacterial growth was completely inhibited by 250 μg/mL SWCNTs and only a slight but not significant cell growth was observed for the *R. solanacearum* cells treated with GO. The antimicrobial activities of SWCNTs, GO and MWCNTs were more efficient in water than in 0.9% NaCl according to Fig. 1B, while the growth curves shown in Fig. 1C suggested that CNMs in 0.1 M PBS did not exhibit any antimicrobial activity against *R. solanacearum* cells. In summary, the above OD growth curves showed that the antibacterial activities of CNMs vary with the type of buffers, which could be attributed to the effects of the ionic strength on the interactions between the bacterial cell and the CNMs [24].

Shown in Fig. 2 are the normalized OD growth curves of *R. solanacearum* cells incubated with different concentrations of SWCNTs. It was found that most of the bacterial killing occurred after 6 h contact with SWCNTs at concentrations of 150–250 μg/mL, while the bacteriostatic activity could be observed at concentrations of 50–100 μg/mL, indicating that the antibacterial activity of SWCNTs was dose-dependent. The growth delay of *R. solanacearum* cells was also assigned to the treatment with GO, and the MWCNTs showed a moderate antibacterial activity (Figs. S2A and S2B). By contrast, rGO and C_{60} did not exhibit significant antibacterial activity toward *R. solanacearum* at a concentration of up to 250 μg/mL (Figs. S2C and S2D). It can be concluded that SWCNTs dispersion shows the highest antibacterial activity, followed by GO, MWCNTs, rGO and C_{60}, respectively.

The difference in the antibacterial activity toward *R. solanacearum* among SWCNTs, MWCNTs, GO, rGO and C_{60} can be attributed to their unique shapes. Needle-like SWCNTs and sharp-knife-like GO exhibit extremely strong antibacterial activity, while ball-like C_{60} did not show significant antibacterial activity. This finding agrees well with a previously published result that triangular silver nanoparticles have better antibacterial activity than spherical and rod-shaped silver nanoparticles [25].

Nevertheless, SWCNTs and GO exhibited stronger antimicrobial activity than MWCNTs and rGO not only due to their unique shapes but also to other properties. One prior study argued that the MWCNTs were much less toxic to bacterial cells than SWCNTs [26]. This difference in activity can also be interpreted by the role that the van der Waals force of SWCNTs and MWCNTs plays in the inactivation of bacterial cells [27]. The stronger Waals force of SWCNTs can induce tight contact between cells and SWCNTs and their needle-like action to cells is more likely to damage the cell walls, whereas the weak Waals force of MWCNTs resulted in loose contacts between cells and MWCNTs and thus

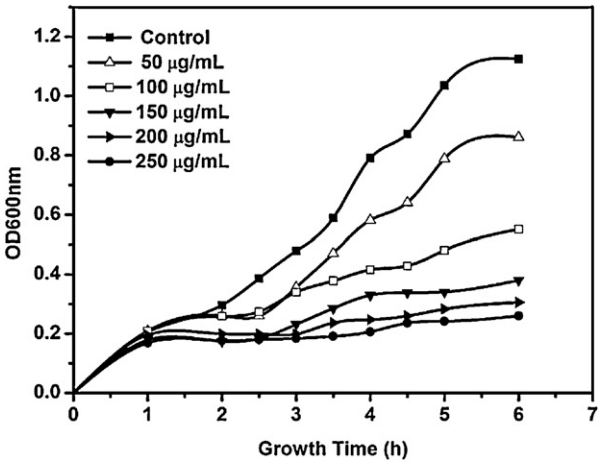

Fig. 2. OD growth curves of *R. solanacearum* in LB broth at 30 °C after the cells (200 μL, 1.2×10^7 cfu/mL) were treated with 50, 100, 150, 200 and 250 μg/mL SWCNTs, respectively, in water for 2 h. Controls were cells untreated with SWCNTs.

less severe cell wall damage. Therefore, a significant difference was observed between the antimicrobial activity of SWCNTs and MWCNTs. Additionally, the difference between the behaviors of GO and rGO observed in TEM images suggests the significant effect of the aggregation/dispersion of graphene-based materials on antibacterial activity. The well-dispersion of GO can be attributed to the large amount of hydrophilic functional groups on GO nanosheets, such as carboxyl, hydroxyl and epoxy groups. However, rGO became hydrophobic after reduction and the strong van der Waals forces made the particles aggregate [19]. As shown in Fig. S1C, the well-dispersed, single-atom-thick and sharp-knife-like GO had more chances to contact bacteria than rGO, thus causing severe damage to cell membrane. Similar results have been reported for *E. coli* inoculated by GO and rGO [28]. Therefore, it can also be concluded that physical properties of CNMs, such as the Waals force, surface functional groups and dispersion state, may determine their antibacterial efficiency against *R. solanacearum*.

These results showed that the antibacterial effect of CNMs not only depends on the type of CNMs, but also on specific conditions such as buffer used, concentrations of CNMs. For the practical application of antibacterial activities of CNMs, the toxicity to plants is a factor that needs to be considered. One of our previous studies have confirmed that MWCNTs aqueous suspension can significantly promote wheat root elongation [14]. Several prior studies have reported that CNTs can stimulate germination and activated enhanced growth in tomato plants, and that CNTs also have the ability to enhance the growth of tobacco cells at concentrations of 100–500 μg/mL [15,29]. The grapheme materials show little or no significant toxicity to some kinds of plants at concentrations of 500–2000 μg/mL [30]. Recently, we have found that the CNMs such as SWCNTs, GO and rGO can promote the germination of tomato seeds and have no significant effect on plant height and root length of tomato plants. Based on our results and prior studies, it can be concluded that in our experimental conditions, the suspensions of CNMs have better antibacterial activity and, at the same time, have positive effects on plants such as growth promotion.

A brief summary can be drawn for the antibacterial activity of CNMs: (1) the shapes of CNMs play an important role in their antibacterial process. (2) The sequence of antimicrobial efficiency is that SWCNTs > GO > MWCNTs, while rGO and C_{60} did not show any antimicrobial activity against *R. solanacearum*. (3) SWCNTs, GO and MWCNTs showed antibacterial activities toward *R. solanacearum* bacterium both in water and in 0.9% NaCl solution, while all five types of nanomaterials showed no significant antimicrobial activity to *R. solanacearum* in 0.1 M PBS.

3.3. Bacterial cell viability after incubation with CNMs

To investigate the antibacterial activity of the CNMs to *R. solanacearum* bacterium, the colony forming count (CFU) method was adopted to determine the cell viability after incubation with CNMs. The lower survival rate indicates the lower activity of the bacterium.

Fig. 3 shows the survival rate of *R. solanacearum* bacterial cells that were treated with different concentrations of SWCNTs and MWCNTs. SWCNTs exhibited a strong antibacterial activity against *R. solanacearum* cells, and the survival rate was only 30–7% after being treated with SWCNTs in water (at a concentration range from 50 μg/mL to 250 μg/mL), obviously suggesting that the higher the concentration of SWCNTs, the lower the survival rates of bacterial cells.

Shown in Fig. 4 is the survival rate of *R. solanacearum* bacterial cells incubated with different concentrations of GO and rGO, which indicates that most of the bacteria could not survive after they were treated with GO in water. In contrast, the rGO did not show any antibacterial activity. The corresponding LB-agar plate images shown in Fig. S4 support the above conclusion. The first vertical panel shows Petri plate images of *R. solanacearum* in the control experiment (untreated with CNMs) after incubation for 48 h. The vertical panels followed show the bacterial growth after being treated with 250 μg/mL SWCNTs, MWCNTs, GO, rGO and C_{60}, respectively. It can be seen from Fig. S4 that the colony number was significantly reduced after being treated with SWCNTs and GO. All these findings are in good agreement with those demonstrated in the OD growth curves.

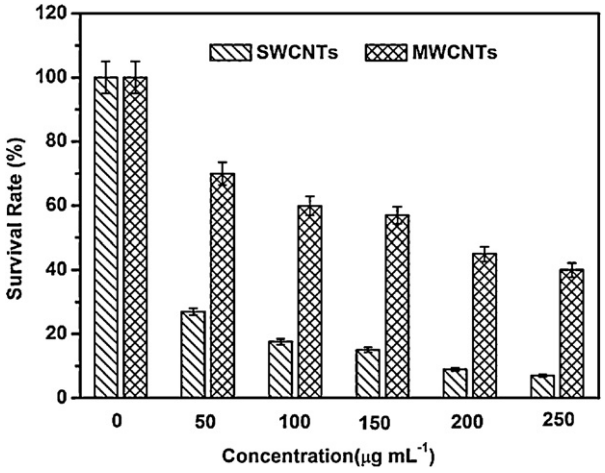

Fig. 3. Cell viability measurements treated with SWCNTs and MWCNTs for 2 h in water. Survival rates were obtained by the colony forming count method. Error bars represent the standard deviation ($n = 4$).

3.4. Fluorescence microscope images of bacterial cells

To verify the reliability of the CFU method, fluorescence microscopy was used to further examine the survival rate of cells after incubation with CNMs dispersions by a Live/Dead bacterial viability kit. DAPI labels live bacteria with blue fluorescence, and PI labels membrane-compromised bacteria with red fluorescence. As SWCNTs and GO showed strong antimicrobial activity to *R. solanacearum* in water, the following assays only focused on the antimicrobial activity of SWCNTs and GO in water. Our fluorescence-based assays showed that cells incubated with SWCNTs and GO for 2 h exhibited a substantial loss in viability (Fig. 5). This result is not only in good agreement with the result obtained

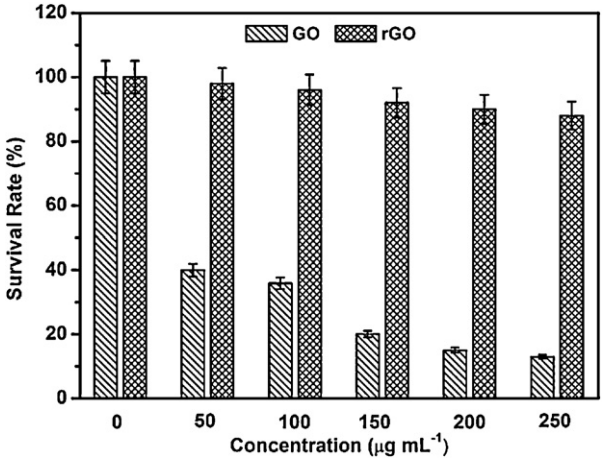

Fig. 4. Cell viability measurements treated with GO and rGO for 2 h in water. Survival rates were obtained by the colony forming count method. Error bars represent the standard deviation ($n = 4$).

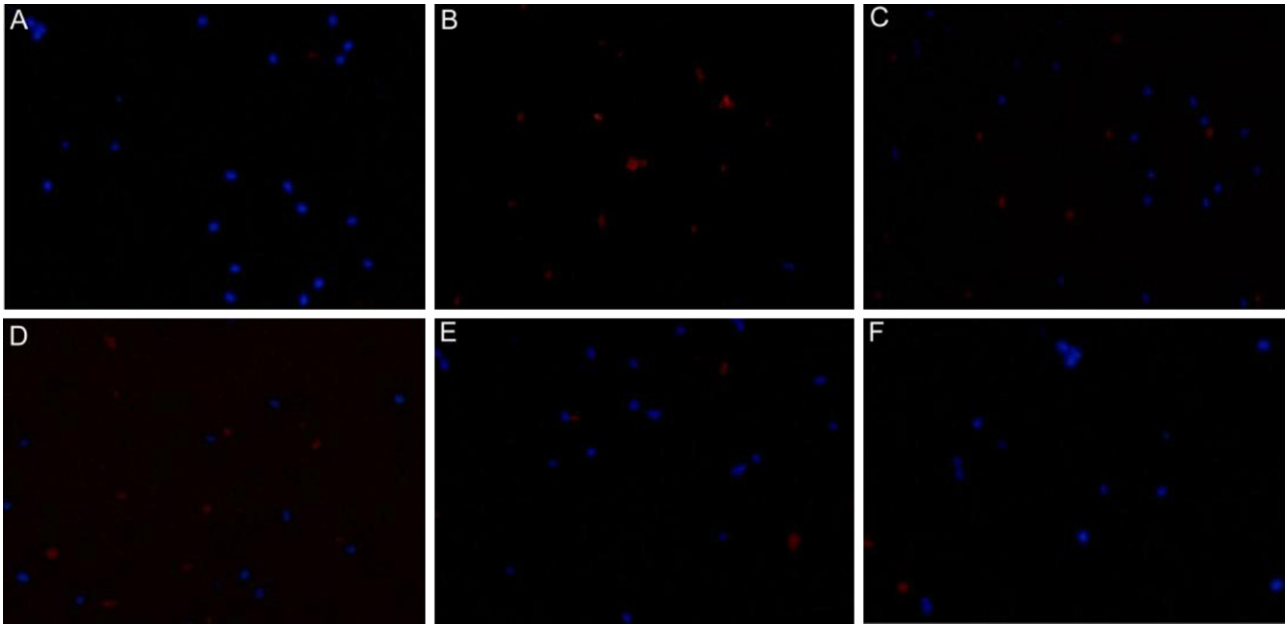

Fig. 5. Cell viability measurements after exposure to aqueous dispersions of CNMs (250 μg/mL). (A) *R. solanacearum* cells in water without CNMs; (B–F) *R. solanacearum* treated with aqueous dispersions of SWCNTs, MWCNTs, GO, rGO and C_{60}, respectively.

by the CFU method, but also suggests that the cell membrane was damaged. The finding was further verified by measuring the intracellular materials of the bacteria.

3.5. Antimicrobial mechanisms of SWCNTs and GO

Experiments were performed to evaluate whether SWCNTs and GO can destroy the cell membrane and induce cell morphological changes. If the cell membrane is compromised, the release of cytoplasmaic constituents, such as DNA and RNA, can be monitored at an optical density of 260 nm. Shown in Fig. 6 is the UV–vis study on the release of 260 nm absorbing materials after the bacteria were incubated with SWCNTs and GO in water. This ratio showed an increase of 1.8 and 1.4 times, respectively. The significant increase in the concentration of plasmid DNA and RNA of the bacteria confirmed that the cell membrane of the bacteria was severely damaged due to the direct contact of the bacteria with SWCNTs and GO. This finding agrees well with a previously published result that SWCNTs caused physical puncture on bacteria, resulting in the

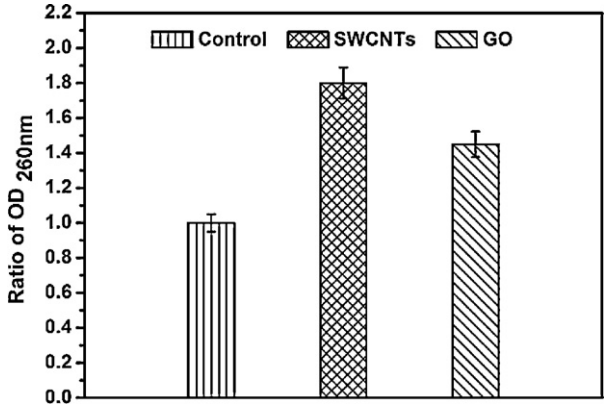

Fig. 6. Release of 260 nm absorbing materials from bacteria treated with aqueous dispersions of SWCNTs and GO, respectively. 100 μL of SWCNTs and GO dispersions (250 μg/mL) was incubated with 1 mL of different bacterial suspensions (10^8 cfu/mL) for 2 h at a 120 rpm shaking speed, and 30 °C. Error bars represent the standard deviation ($n = 4$).

physical damages of the outer membrane of the cells [9]. The damage of bacterial membrane was further verified by SEM and TEM imaging.

Fig. 7 shows the morphological changes of the *R. solanacearum* bacterium after incubation with SWCNTs or GO. It was observed under our experimental conditions (Fig. 7A) that the *R. solanacearum* bacterium in water without CNMs maintained the integrity of the membrane structure. In contrast, the majority of the cells lost their cellular integrity and became elongated or flattened after being incubated with SWCNTs or GO (Fig. 7B and C). The TEM images of the bacterium obtained after incubation with SWCNTs or GO (Fig. 7D–F) indicate that irreversible damages to cell membrane could be induced by SWCNTs or GO and then the cytoplasm of the bacterial cells released resulted in the viability loss of a large fraction of cells, which is in agreement with SEM imaging. These results have confirmed that cell membrane was damaged after direct contact with SWCNTs and GO. Thus, the bactericidal activity of SWCNTs and GO could be due to (i) the close contact of bacteria with the SWCNTs and GO and/or (ii) the release of cytoplasmaic constituents after cell membrane was damaged by SWCNTs and GO.

The copious use of copper-based bactericides in agriculture for the control of bacterial pathogens has led to the development and prevalence of copper-resistant strains in pathogen populations affecting plants [31]. It is well established that the mechanisms of copper resistance determinants have been localized to plasmid DNA, which is also related to the chromosomally encoded systems for uptake and management of trace levels of copper [32]. However, our results suggest that the bactericidal action mode of SWCNTs and GO is physical puncture on bacteria, degrading the bacterial cell integrity and causing the cell death. Thus, these resistant bacteria can be overcome by SWCNTs and GO with distinct antibacterial properties. Moreover, it is well known that almost all plant pathgenic bacteria, whether copper-resistant strains or non-resistant bacterial pathogens, are Gram-negative bacteria and have the same cell wall structure. The difference between copper-resistant strains and non-resistant bacterial pathogens is the molecular resistant mechanism toward the copper pesticides. As a corollary, SWCNTs and GO can have anti-bacterial effects not only on resistant bacterial pathogens but also on non-resistant bacterial pathogens, and

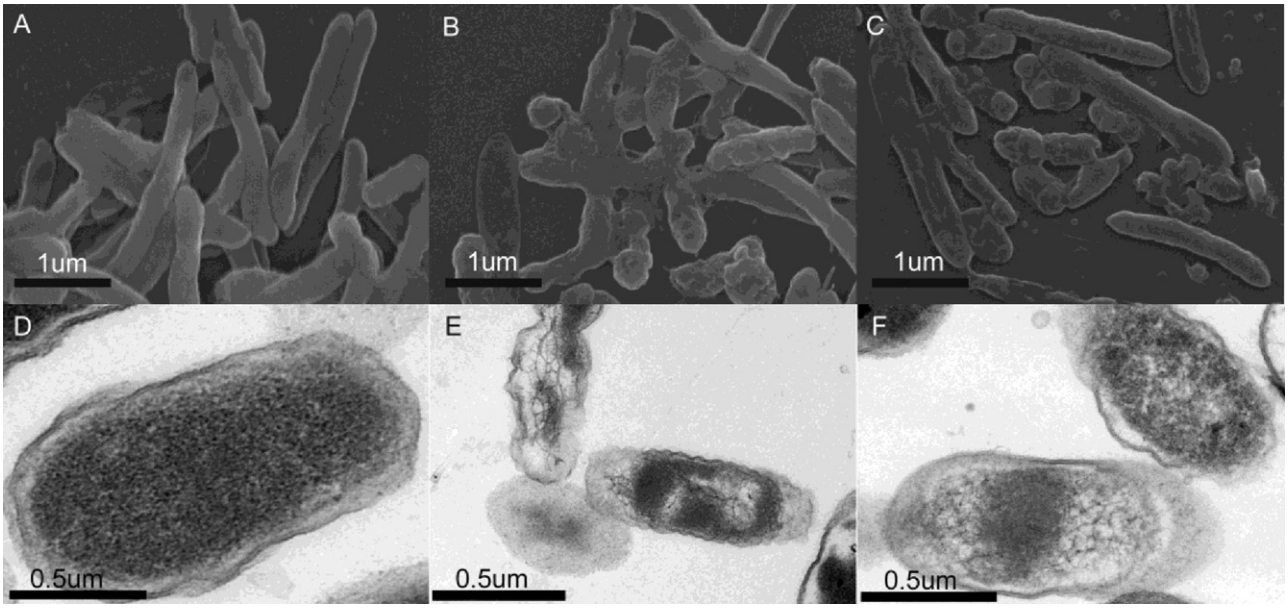

Fig. 7. SEM images of *R solanacearum* cells treated (A) without CNMs, (B) with SWCNTs, and (C) with GO suspensions, respectively. TEM images of *R. solanacearum* cells treated (D) without CNMs, (E) with SWCNTs, and (F) with GO suspensions,respectively. 100 μL of SWCNTs and GO dispersion (250 μg/mL) was incubated with 1 mL of different bacterial suspensions (10^8 cfu/mL) for 2 h at a 120 rpm shaking speed, and 30 °C.

this in vitro bactericidal activity suggests potential applications in counteracting the bacterial resistance.

4. Conclusions

The tremendous resistance of plant pathogen bacteria to conventional bactericidal agents has prompted many studies on novel antibacterial materials that can limit the bacterial growth or completely kill them in plant protection. In this work, we demonstrated the significant antibacterial activities of CNMs such as SWCNTs and GO against copper-resistant *R. solanacearum* bacteria. The antibacterial mechanism of SWCNTs and GO is shown to be attributed to the destruction of cell membrane and the release of cytoplasm. The antibacterial activity of SWCNTs and GO may apply to both resistant and non-resistant bacterial pathogens. Future studies are supposed to include other important agricultural bacteria in bioassay to extend the spectrum of CNMs anti-plant pathogenic bacteria activities. The fundamental investigations on the antimicrobial activity of CNMs have contributed as building blocks to the construction of the basis for extending the potential application of CNMs as antimicrobial materials in plant protection.

Acknowledgements

The authors gratefully acknowledge the support for this research by National Natural Science Foundation of China (20975042, 21175051), the Fundamental Research Funds for the Central Universities of China (2010PY009, 2011PY139) and the Natural Science Foundation of Hubei Province Innovation Team (2011CDA115).

Appendix A. Supplementary data

Supplementary data associated with this article can be found, in the online version, at http://dx.doi.org/10.1016/j.colsurfb.2012.09.044.

References

[1] F. Bertolla, F.V. Gijsegem, X. Nesme, P. Simonet, Appl. Environ. Microbiol. 63 (1997) 4965–4968.
[2] J.M. Colburn-Clifford, J.M. Scherf, C. Allen, Appl. Environ. Microbiol. 76 (2010) 392–7399.
[3] M. Sylvie, E. Badosa, E. Besalu, M. Planas, E. Bardaji, E. Montesinos, L. Feliu, Peptides 27 (2006) 2575–2584.
[4] G.W. Sundin, C.L. Bender, Appl. Environ. Microbiol. 59 (1993) 1018–1024.
[5] I. Fock, C. Collonnier, A. Purwito, J. Luisetti, V. Souvannavong, F. Vedel, A. Servaes, A. Ambroise, H. Kodja, G. Ducreux, Plant Sci. 160 (2000) 165–176.
[6] P. Pradhanang, P. Ji, M. Momol, S. Olson, J. Mayfield, J. Jones, Plant Dis. 89 (2005) 989–993.
[7] J.C. Hong, M.T. Momol, P. Ji, S.M. Olson, J. Colee, J.B. Jones, Crop Prot. 30 (2011) 1340–1345.
[8] S.B. Liu, T.H. Zeng, M. Hofmann, E. Burcombe, J. Wei, R. Jiang, J. Kong, Y. Chen, ACS Nano 5 (2011) 6971–6980.
[9] S.B. Liu, L. Wei, L. Hao, N. Fang, M.W. Chang, R. Xu, Y. Yang, Y. Chen, ACS Nano 3 (2009) 3891–3902.
[10] S. Kang, M.S. Mauter, M. Elimelech, Environ. Sci. Technol. 42 (2008) 7528–7534.
[11] W. Hu, C. Peng, W. Luo, M. Lv, X. Li, D. Li, Q. Huang, C. Fan, ACS Nano 4 (2010) 4317–4323.
[12] K.S. Brammer, C. Choi, C.J. Frandsen, Acta Biomater. 7 (2011) 2697–2703.
[13] T.J. Simmons, S.H. Lee, T.J. Park, D.P. Hashim, P.M. Ajayan, R.J. Linhardt, Carbon 47 (2009) 1561–1564.
[14] X.P. Wang, H.Y. Han, X.Q. Liu, X.X. Gu, K. Chen, D.L. Lu, J. Nanopart. Res. 14 (2012) 841–850.
[15] M.V. Khodakovskaya, K. Silva, D.A. Nedosekin, E. Dervishic, A.S. Birisa, E.V. Shashkov, E.I. Galanzha, V.P. Zharov, Proc. Natl. Acad. Sci. U.S.A. 108 (2011) 1029–1033.
[16] S. Kang, M. Pinault, L.D. Pfefferle, M. Elimelech, Langmuir 23 (2007) 8670–8673.
[17] D.Y. Lyon, L. Brunet, G.W. Hinkal, M.R. Wiesner, P.J.J. Alvarez, Nano Lett. 8 (2008) 1539–1543.
[18] J.W.S. Hummers, R.E. Offeman, J. Am. Chem. Soc. 80 (1958), 1339–1339.
[19] S. Stankovich, D.A. Dikin, R.D. Piner, K.A. Kohlhaas, A. Kleinhammes, Y. Jia, Y. Wu, S.T. Nguyen, R.S. Ruoff, Carbon 45 (2007) 1558–1565.
[20] W.B. Hu, C. Peng, W.J. Luo, M. Lv, X.M. Li, D. Li, Q. Huang, C.H. Fan, ACS Nano 4 (2010) 4317–4323.
[21] K.S. Brammer, C. Choi, C.J. Frandsen, O. Seunghan, G. Johnston, S.H. Jin, Acta Biomater. 7 (2011) 2697–2703.
[22] Y. Bai, I.S. Park, S.J. Lee, P.S. Wen, T.S. Bae, M.H. Lee, Colloids Surf. B: Biointerfaces 89 (2012) 101–107.
[23] H.Z. Zardini, A. Amiri, M. Shanbedi, M. Maghrebi, M. Baniadam, Colloids Surf. B: Biointerfaces 92 (2012) 196–202.
[24] H.H. Liao, R.L. Qi, M.W. Shen, X.Y. Cao, R. Guo, Y.Z. Zhang, X.Y. Shi, Colloids Surf. B: Biointerfaces 84 (2011) 528–535.

[25] S. Pal, Y.K. Tak, J.M. Song, Appl. Environ. Microbiol. 73 (2007) 1712–1720.
[26] L.R. Arias, L. Yang, Langmuir 25 (2009) 3003–3012.
[27] S. Kang, M. Herzberg, D.F. Rodrigues, M. Elimelech, Langmuir 24 (2008) 6409–6413.
[28] S. Liu, T.H. Zeng, M. Hofmann, E. Burcombe, J. Wei, R. Jiang, J. Kong, Y. Chen, ACS Nano 5 (2011) 6971–6980.
[29] M.V. Khodakovskaya, K. Silva, A.S. Biris, E. Dervishi, H. Villagarcia, ACS Nano 6 (2012) 2128–2135.
[30] P. Begum, R. Ikhtiari, B. Fugetsu, Carbon 49 (2011) 3907–3919.
[31] H.J. Scheck, J.W. Pscheidt, Plant Dis. 82 (1998) 397–406.
[32] D.A. Cooksey, Mol. Microbiol. 7 (1993) 1–5.